

Grain refinement of AM60/Al₂O_{3p} magnesium metal-matrix composites processed by ECAE

S.-J. Huang¹, P.-C. Lin^{2*}

¹*Department of Mechanical Engineering, National Taiwan University of Science and Technology, 43, Sec. 4, Keelung Rd., Taipei, 106, Taiwan, ROC*

²*Department of Mechanical Engineering, National Chung Cheng University, 168 University Rd., Ming-Hsiung, Chia-Yi, 621, Taiwan, ROC*

Received 23 May 2012, received in revised form 28 March 2013, accepted 28 March 2013

Abstract

This paper studies the mechanical properties enhancement of AM60/Al₂O_{3p} magnesium metal-matrix nanocomposites by equal channel angular extrusion (ECAE) that is a useful technique to produce bulk nano-structured materials by severe plastic deformation. The present magnesium metal matrix composites (Mg MMCs) with 1, 2 and 5 wt.% of nano-sized Al₂O₃ particulates for ECAE were fabricated using stir-casting method. Observing the microstructures of MMCs, the more uniform microstructure consisting of grains with an average grain size of ~ 0.8 μm was observed in the AM60/5wt.%Al₂O_{3p} MMC after 4 passes. The hardness of MMCs increases evidently with the increase of the weight percentage of Al₂O_{3p} additions and ECAE passes. The optimal hardness of AM60/5wt.%Al₂O_{3p} MMC after 4 passes increased to 103.7 HV, which is by 87.2 % higher than that of as-cast AM60.

Key words: grain refinement, ECAE, metal matrix composites, magnesium alloy, nano-scaled aluminum oxide

1. Introduction

Magnesium (Mg) alloys are gaining more recognition as the lightest structural material for light-weight applications, due to their low density and high stiffness-to-weight ratio. Even so, Mg alloys have not been used for critical performance applications because of their inferior mechanical properties compared to other engineering materials. Hence, many researchers attempt to fabricate Mg-based metal-matrix composites (Mg MMCs) by different methods to obtain light-weight materials with excellent mechanical properties [1–7].

In order to improve the quality of MMCs, a method preserving high technological ductility with efficient and multiple strength enhancements has been developed on the basis of severe plastic deformation (SPD) technique [8]. This method enables manufacturing high-strength bulk billets out of metallic materials. One of the SPD techniques is the equal channel angular extrusion (ECAE) [9]. This strength en-

hancement technique aims at maximum refinement of the grain structure down to submicrocrystalline- and nano-scale.

In recent years, ceramic nanopowders have been used to reinforce metallic materials. According to the Orowan strengthening mechanism, finer particles are more efficient to improve the mechanical properties. Regarding to the fabrication of Mg MMCs, Hassan et al. [10, 11] applied it to prepare the composite of pure magnesium by adding reinforcement phase Al₂O₃ with different particle sizes and weight percentages. The result showed that the hardness and ductility would increase apparently when the reinforcement phase particle was 50 nm. And nano-Al₂O_{3p} also significantly refined grains of magnesium matrix when added in higher weight percentage. Paramsothy et al. [12, 13] reported AZ31 nanocomposite containing Al₂O₃ nanoparticle reinforcement being fabricated using solidification processing followed by hot extrusion. The AZ31 nanocomposite exhibited slightly smaller grain sizes than monolithic AZ31, and 30 %

*Corresponding author: tel.: +886933598770; e-mail address: fsix01122000@gmail.com

higher hardness than monolithic AZ31. Habibnejad-Korayem et al. [14] studied 0.5, 1 and 2 wt.% of alumina nano-particles being added to pure Mg and AZ31 magnesium alloy via a stir-casting method. A uniform distribution of the nano- Al_2O_3 with an average diameter of 100 nm could refine the grain structure of cast materials. Chen et al. [15] reported AZ91D magnesium alloy being grain refined by SiC particles. The results indicated that SiC particle was an effective grain refiner for AZ91D alloy and could decrease the grain size under an optimized refining technology.

There were not so many researchers investigating AM60 Mg MMCs after ECAE. Semenov et al. [16] presented the tribological contact characteristics of R18 tool steel in the interface with AZ91D magnesium alloy hardened with SiC dispersed powder filler and by severe plastic deformation (SPD) – specifically, equal channel angular pressing (ECAP). SPD was shown to enhance efficiently the strength of the original material due to its grain structural refinement that considerably influenced the reduction in adhesive component of the friction coefficient. Jiang Jufu et al. [17] studied AM60 magnesium alloy semisolid slurry being prepared by new strain induced melt activated (new SIMA). The results showed that the microstructure was well refined to fine equiaxed grains with the average size of $8\ \mu\text{m}$ after the process of as-cast AM60 magnesium alloy by ECAE.

From previous studies, it is found that the Mg MMCs using different kinds of particles can refine the grain size. Mg MMCs generally exhibit poor workability because of HCP structure. Therefore, it is required to improve poor workability of Mg MMCs for the development of plastic forming technology by ECAE. But the research of AM60 MMCs added with nano-scale Al_2O_3 particle and extruded by ECAE is not adequate. This study selects nano-scale Al_2O_3 particle material as the reinforcement particle and, using the melt stirring technique, to integrate the reinforcement particles into AM60 melt to form AM60 MMCs. Finally, the properties of Mg MMCs are improved by different ECAE passes to obtain the best mechanical properties.

2. Experimental details

2.1. Materials preparation

The matrix used in this work is magnesium alloy AM60 with $\sim 6.0\%$ aluminum. Its chemical composition is shown in Table 1. Al_2O_3 particles with weight fraction of 1, 2, and 5 % within MMCs are used as the reinforcement phase. The commercially available Al_2O_3 powder with a particle diameter about 25 nm, purity of $\geq 99.8\%$ is added into AM60 to form Mg-based metal matrix composites.

Table 1. Chemical composition of AM60

Elements	Al	Mn	Zn	Si	Fe	Cu	Ni	Mg
wt.%	5.8	0.32	0.22	0.1	0.005	0.01	0.002	Balance

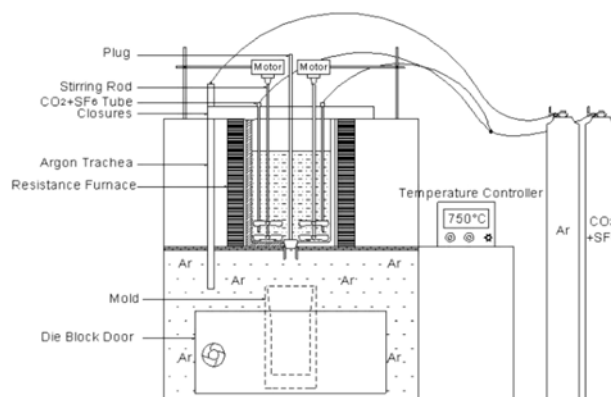


Fig. 1. Setup configuration.

The melt-stirring technique was used for fabricating the present Mg MMCs. Experimental setup is shown in Fig. 1. The AM60 was initially placed inside a graphite crucible and heated to 750°C in a resistance-heated furnace. The molten alloy was stirred with a vane operated at $450\ \text{rev}\ \text{min}^{-1}$ for 10 min. Preheated Al_2O_3 particles were simultaneously added to the stirred alloy. Then the composite melt was finally poured into a metallic mold. The AM60 MMCs containing Al_2O_3 with different weight fraction of 1, 2, and 5 wt.% were prepared for further mechanical testing. The AM60 MMCs were homogenized at 410°C for 18 h and water quenched. These ingots were hot extruded by an extrusion ratio of 12.25 : 1 on a 500 ton hydraulic extruder. Extrusion was carried out at 360°C . The preformation was held at 360°C for 90 min in a constant temperature furnace before extrusion. Colloidal graphite was used as the lubricant. Rods with 20 mm diameter were obtained as the following extrusion. Billets of $11.4 \times 11.4 \times 95\ \text{mm}^3$ were processed from AM60 and AM60 MMCs rods, which were prepared for ECAE process.

2.2. ECAE process

The scheme of ECAE shown in Fig. 2 was carried out in a die with the die angle $\Phi = 120^\circ$ and the outer die angle $\Psi = 0^\circ$. The extrusion temperature was controlled within $\pm 5^\circ\text{C}$ of the setting temperature, and the extrusion temperature was set at 270°C . During the extrusion, the plunger speed was about

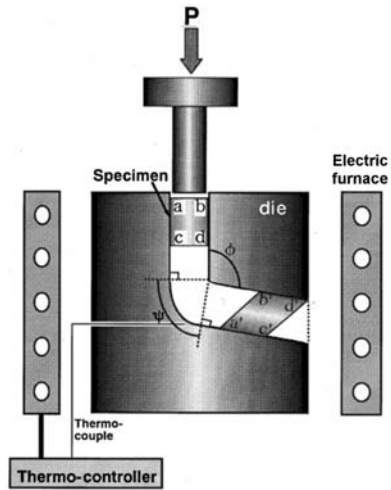


Fig. 2. The scheme of ECAE.

0.7 mm s^{-1} . After each extrusion pass, the billet was quenched into water. The billet was rotated counter-clockwise about the exit extrusion axis by 90° between

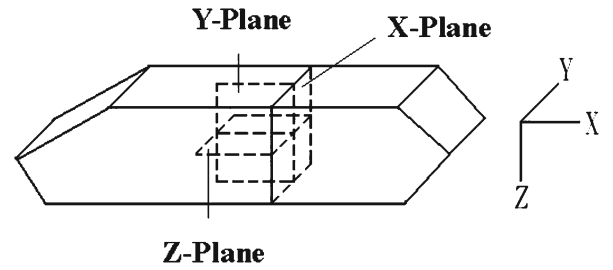


Fig. 3. Sampling position of microstructure and hardness test.

each pass, the so-called route Bc [18], and each billet was extruded 1, 2 and 4 times.

2.3. Metallographic observations and hardness tests

The microstructures of AM60 and AM60/ $\text{Al}_2\text{O}_3\text{p}$ MMC after ECAE specimens were observed by an optical microscope. Microstructural characterization studies were conducted on metallographically pol-

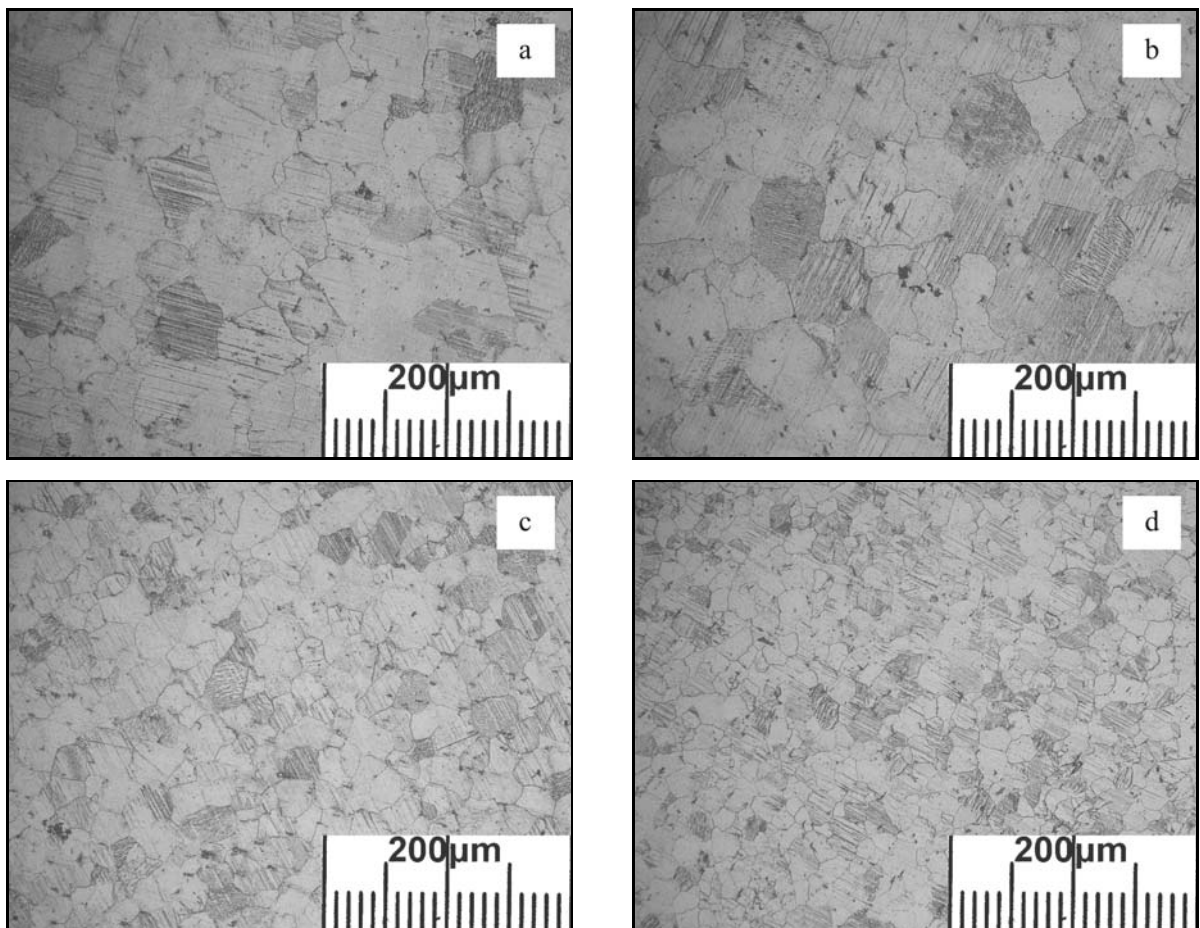


Fig. 4. Microstructure of as-cast: (a) AM60, (b) AM60/1wt.% $\text{Al}_2\text{O}_3\text{p}$, (c) AM60/2wt.% $\text{Al}_2\text{O}_3\text{p}$, (d) AM60/5wt.% $\text{Al}_2\text{O}_3\text{p}$; $100\times$.

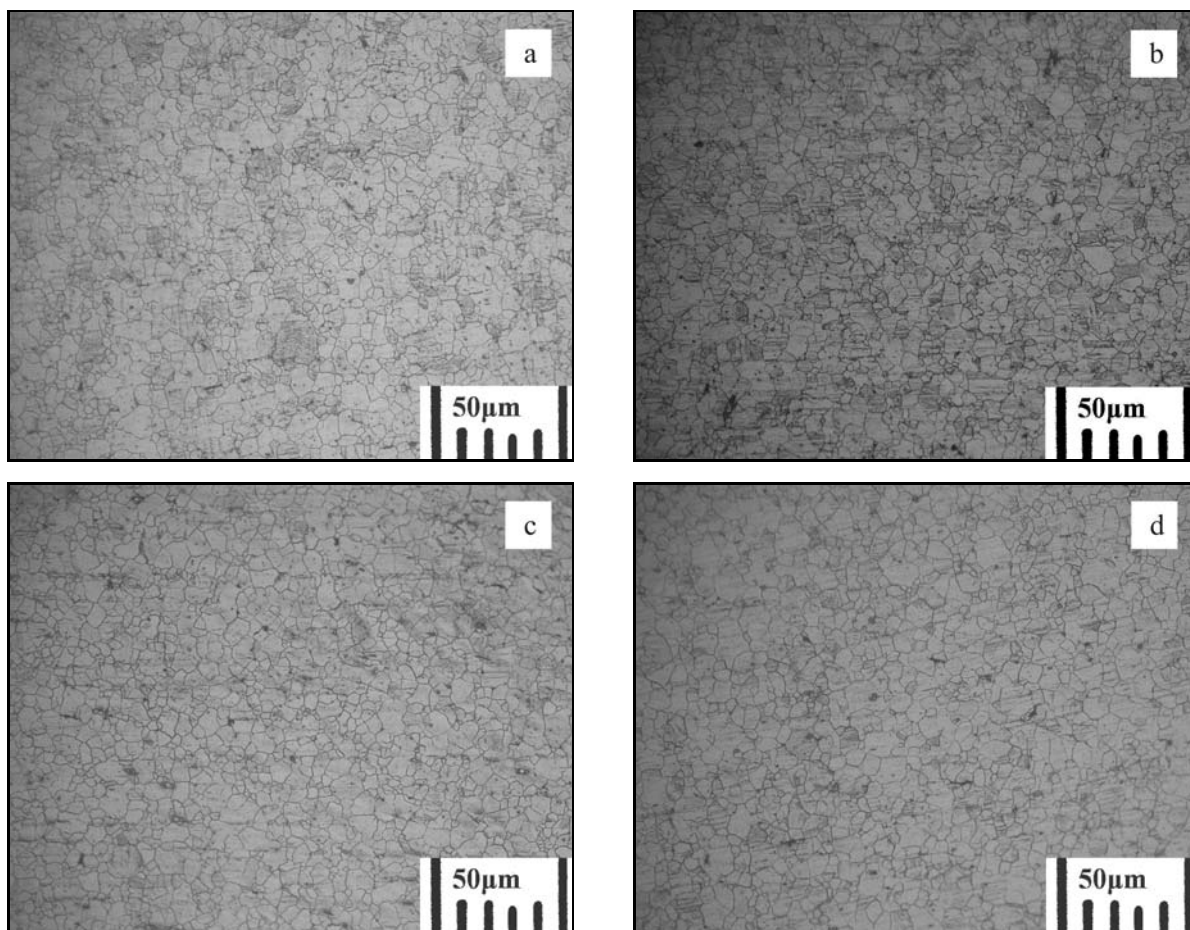


Fig. 5. Microstructure of billet (ECAE, $N = 0$): (a) AM60, (b) AM60/1wt.%Al₂O_{3p}, (c) AM60/2wt.%Al₂O_{3p}, (d) AM60/5wt.%Al₂O_{3p}; 500 \times .

Table 2. Variation of average grain size (μm) with number of ECAE passes in AM60 and AM60 MMC

TYPE	AM60	AM60 + 1wt.%Al ₂ O _{3p}	AM60 + 2wt.%Al ₂ O _{3p}	AM60 + 5wt.%Al ₂ O _{3p}
As-cast	97.5	55.3	45.6	37.4
*ECAE, $N = 0$	18.2	14.7	14.3	12.2
ECAE, $N = 1$	12.4	9.7	8.3	6.4
ECAE, $N = 2$	5.4	4.5	2.5	2.1
ECAE, $N = 4$	4.2	3.2	1.5	0.8

*Billet without ECAE

ished ECAEed MMCs to investigate the morphological characteristics of grains. The mean grain size was determined using the linear intercept method. With a load of 300 gf, Vickers microhardness measurements were carried out on AM60 and AM60/Al₂O_{3p} MMCs with a Matsuzawa (Model MV-1) hardness tester. The average hardness of each as-cast AM60 and AM60 MMC was obtained from 10 tests.

The test sheet with ECAE was observed in the X, Y, Z planes, as shown in Fig. 3. Furukawa et al. [19] indicated that the extrusion with Route Bc had the shear strain angle on X-plane change larger than that on the rest two planes. The shear strain effect is

therefore more significant, benefiting the discussions between microstructures and hardness.

3. Results and discussion

3.1. Metallographic observations

Figure 4 shows typical optical microstructures at the centre of the examined cross sections of the as-cast ingots of AM60 MMCs with different weight percentages of Al₂O_{3p}. From Fig. 4, the addition of Al₂O_{3p} reduces the grain size from 97.5 μm to 37.4 μm . Fig-

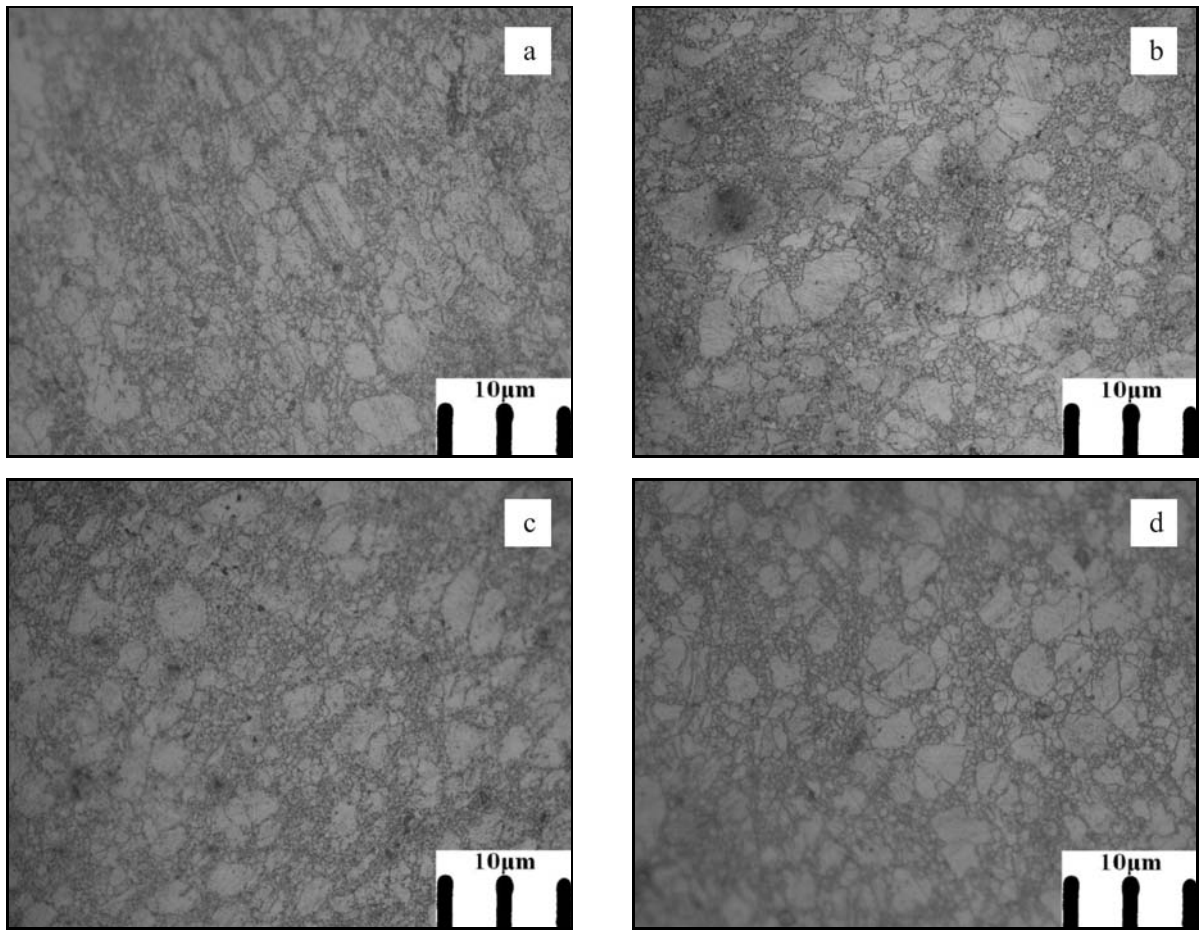


Fig. 6. Microstructure of billet (ECAE, $N = 1$): (a) AM60, (b) AM60/1wt.%Al₂O_{3p}, (c) AM60/2wt.%Al₂O_{3p}, (d) AM60/5wt.%Al₂O_{3p}; 500 \times .

ures 5–8 show the microstructures of the MMCs extruded at different ECAE passes, and the average grain size data of the MMCs as a function of ECAE pass are listed in Table 2 and shown in Fig. 9. From Figs. 4 and 5, when Mg-based metal matrix composites were extruded into rods, the microstructures were comparatively even and the particle size of rods was about 10–20 μm . Figures 6 and 7 show the uneven microstructures of particles after the refinement of particles with one and two ECAE passes. Figure 8 shows even and fine microstructures of particles after four ECAE passes. From Fig. 9, the average grain sizes of MMCs decreased evidently with an increase of the weight percentages of Al₂O_{3p} additions and ECAE passes. A more uniform microstructure consisting of grains with an average grain size of $\sim 0.8 \mu\text{m}$ was observed in AM60/5wt.%Al₂O_{3p} MMC after 4 passes (Fig. 8d). In the case of ECAEed AM60 MMCs, the grain growth restriction might have been preferred by the presence of nano-Al₂O_{3p}. During the ECAE process, dynamic recrystallization and grain growth were likely to occur in order to reduce grain size of materials. However, nano-Al₂O_{3p} would help in reducing the grain size by the particle stimulated nucle-

ation (PSN) mechanism [20]. Furthermore, the pinning effect of these particles can oppose grain growth by reducing the grain boundary migration [21]. These two phenomena together with the partitioning of the grains imposed by the severe plastic deformation in the ECAE process have all contributed to the achieved fine-grained structure in the AM60 MMCs. In the deformation, the rods appear plastic deformation at the turning point of mold at 270 $^{\circ}\text{C}$. With the rapid increase of shear strain, the temperature would produce dynamic recrystallization to form new crystalline grains when completing the plastic deformation. The above descriptions are the factors in refinement of crystalline grains.

3.2. Hardness

Table 3 presents the results of the microhardness measurement conducted on as-cast AM60 and AM60/Al₂O_{3p} MMC after different passes, revealing an increase in MMCs hardness with an increase in weight percentage of nano-Al₂O_{3p}. The hardness data of the MMCs as a function of ECAE passes are shown in Fig. 10. The optimal hardness appears at

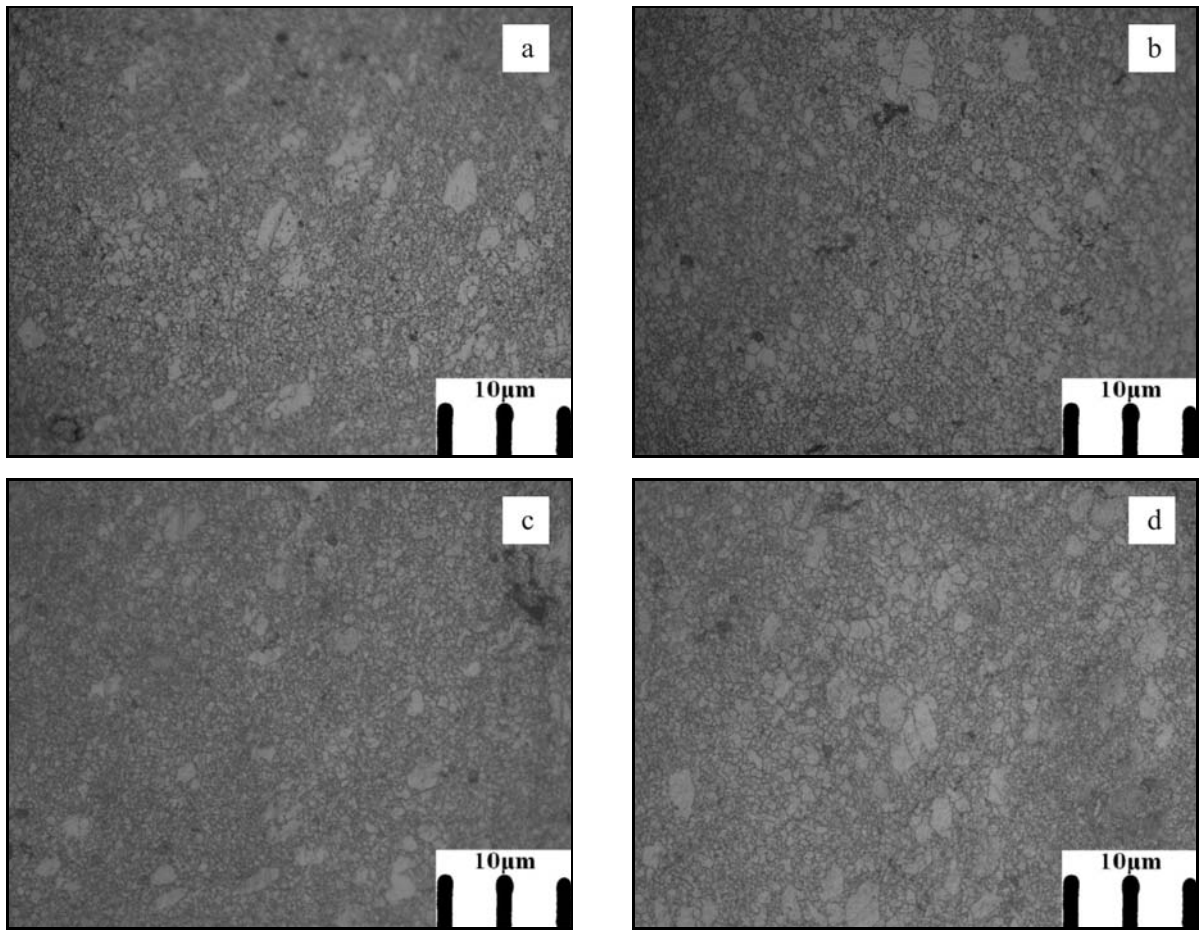


Fig. 7. Microstructure of billet (ECAE, $N = 2$): (a) AM60, (b) AM60/1wt.%Al₂O_{3p}, (c) AM60/2wt.%Al₂O_{3p}, (d) AM60/5wt.%Al₂O_{3p}; 500 \times .

Table 3. Variation of microhardness, HV, with number of ECAE pass in AM60 and AM60 MMC

TYPE	AM60	AM60 + 1wt.%Al ₂ O _{3p}	AM60 + 2wt.%Al ₂ O _{3p}	AM60 + 5wt.%Al ₂ O _{3p}
As-cast	55.4	56.8	58.1	61.7
*ECAE, $N = 0$	63.3	66.9	68.5	72.8
ECAE, $N = 1$	79.9	83	86.6	92.5
ECAE, $N = 2$	86	91	93.4	99.4
ECAE, $N = 4$	92.1	94.4	97.2	103.7

*Billet without ECAE

AM60/5wt.%Al₂O_{3p} MMC after 4 passes, and the maximum hardness is 103.7 HV. From Fig. 11, the hardness increases with the decreasing average grain size. The relationship of grain refinement and hardness could be discussed on the basis of the Hall-Petch equation [22]:

$$H = H_0 + k_H d^{-1/2}, \quad (1)$$

where H is hardness, d is the matrix grain diameter and k_H is the Hall-Petch coefficient. From formula (1), when d gets smaller, the material becomes harder so that the refinement of crystalline

grains could effectively enhance the hardness of materials. Moreover, nano-Al₂O_{3p} being evenly distributed in Mg alloy could be regarded as the barrier to the movement of dislocation to achieve the effect of dispersion hardening. Comparing Table 2 with Table 3, the hardness of AM60/5wt.%Al₂O_{3p} MMC had 15 % increase more than that of AM60. Furthermore, the hardness of AM60/5wt.%Al₂O_{3p} MMC after 4 passes had 68 % increase more than that of AM60/5wt.%Al₂O_{3p} MMC. Hence, the hardness of Mg alloy can be improved both by adding reinforcement particles (Orowan strengthening) and ECAEed grain refinement (Hall-Petch strengthening accompan-

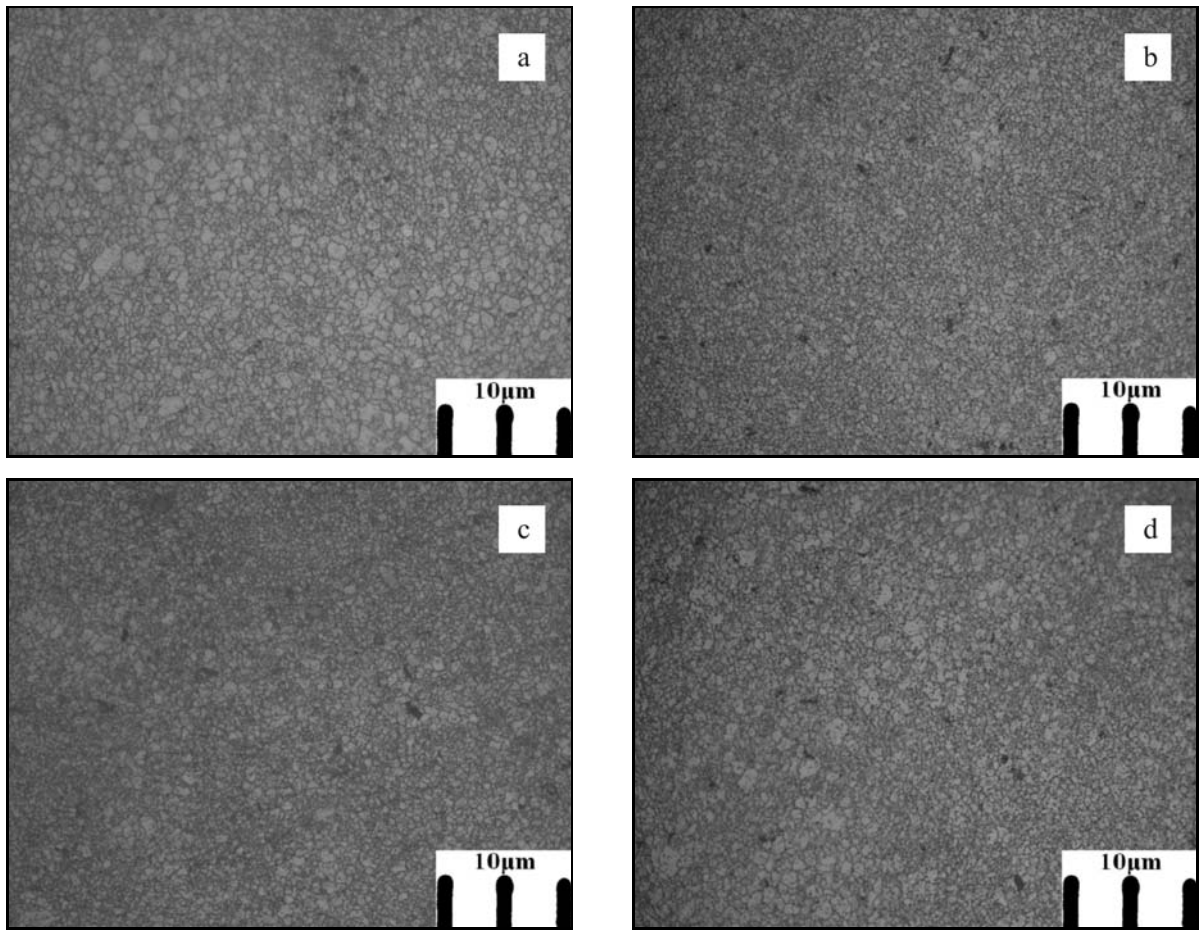


Fig. 8. Microstructure of billet (ECAE, $N = 4$): (a) AM60, (b) AM60/1wt.%Al₂O_{3p}, (c) AM60/2wt.%Al₂O_{3p}, (d) AM60/5wt.%Al₂O_{3p}; 500 \times .

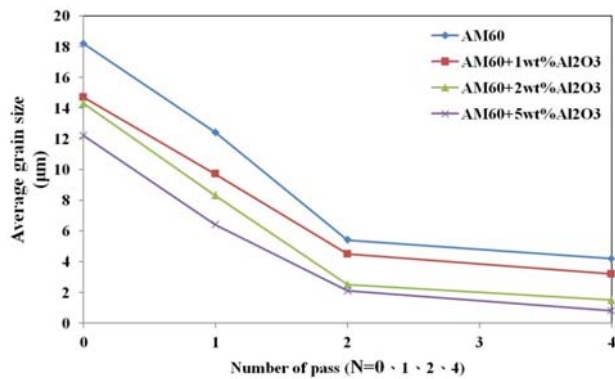


Fig. 9. Variation of average grain size with number of ECAE passes in AM60 and AM60 MMC.

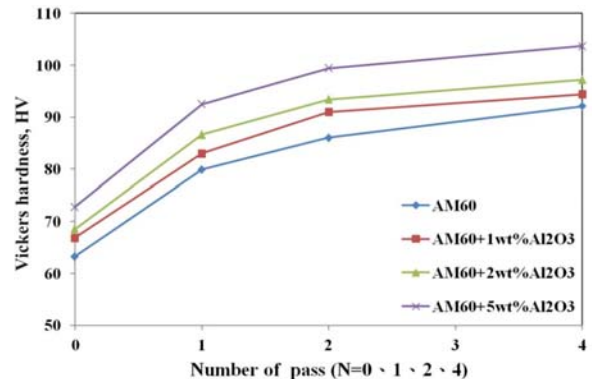


Fig. 10. Variation of microhardness with number of ECAE passes in AM60 and AM60 MMC.

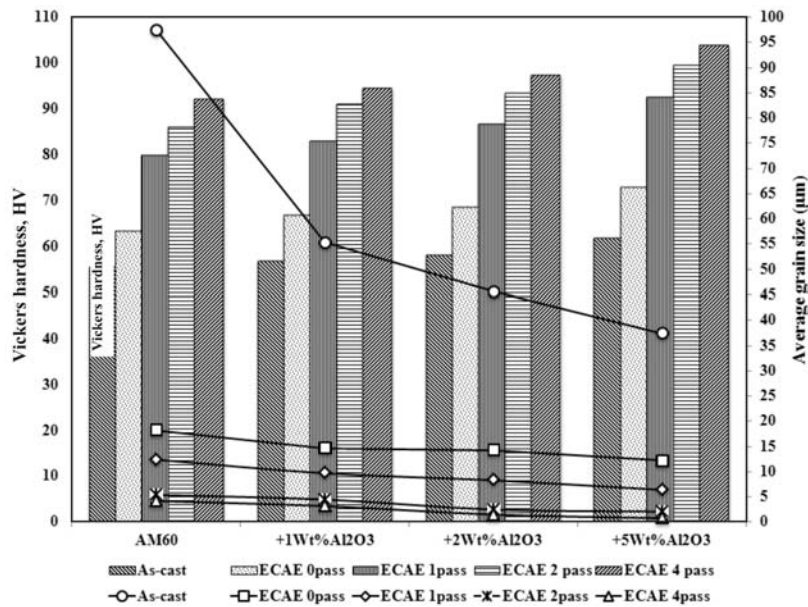
ied with dislocation density increase strengthening). But the contribution of ECAEed fine grain strengthening was higher than that of dispersion strengthening effect. Besides, there is another strengthening mechanism existing during high temperature process, i.e., dislocation density increase strengthening, which will be discussed and compared with former two mechanisms in the next section.

3.3. Strengthening mechanism contribution

For all alloy composites, the addition of Al₂O₃ nanoparticles significantly increased hardness. The AM60/5wt.%Al₂O_{3p} MMC after 4 passes had the highest increase in hardness relative to the matrix of the composite tested. The mechanisms of strengthening have been studied recently. Typically, three

Table 4. Parameters used to determine predicted strengthening enhancement for AM60/5wt.%Al₂O₃ MMC after 4 passes

Parameter	Description	Value	Reference/note
α_m	coefficient of thermal expansion of the matrix	$25.5 \times 10^{-6} \text{ }^\circ\text{C}^{-1}$	–
α_p	coefficient of thermal expansion of the nanoparticles	$7.4 \times 10^{-6} \text{ }^\circ\text{C}^{-1}$	–
β	dislocation strengthening coefficient	1.25	[27]
b	magnitude of the burgers vector	0.32 nm	[28]
d_c	average grain size in the composite sample	0.8 μm	experimentally determined
d_m	average grain size in the monolithic sample	97.5 μm	experimentally determined
d_p	nanoparticle diameter	25 nm	manufacture supplied average particle size
G_m	shear modulus of the matrix	14.8 GPa	calculation and experimentally determined
k_y	Hall-Petch material constant	$0.097 \text{ MPa}\sqrt{\text{m}}$	calculation and experimentally determined
T_{process}	processing temperature	270 $^\circ$	–
T_{test}	testing temperature	25 $^\circ$	–
V_p	volume fraction of nanoparticles	0.0365	calculated from weight fraction

Fig. 11. The relationship of average grain size and hardness of AM60-Al₂O₃ MMCs with wt.% of Al₂O₃.

strengthening mechanisms are proposed to explain the strength enhancement in MMCs. They are: enhanced dislocation density in the matrix due to thermal expansion mismatch [23], Hall-Petch strengthening due to a refined grain structure [24], and Orowan strengthening [25]. These can be calculated as

$$\Delta\sigma_D = \sqrt{3}\beta G_m b \sqrt{\frac{12(T_{\text{process}} - T_{\text{test}})(\alpha_m - \alpha_p)V_p}{bd_p}}, \quad (2)$$

$$\Delta\sigma_{\text{Hall-Petch}} = k_y \left(d_m^{-1/2} - d_c^{-1/2} \right), \quad (3)$$

$$\Delta\sigma_{\text{Orowan}} = \frac{0.13G_m b}{d_p \left[\left(\frac{1}{2V_p} \right)^{1/3} - 1 \right]} \ln \frac{d_p}{2b}, \quad (4)$$

where the parameters of these expressions for AM60/5wt.%Al₂O₃ MMC after 4 passes are shown in Table 4.

Let us assume that the hardness is proportional to the yield strength [26]. Table 5 shows the contribution of above mentioned three mechanisms to the strength of composites, respectively. From the calculation results of strength increase, it can be found that the hardness increase contribution of the dislocation density increase strengthening (56 %) is larger than the Hall-Petch (34 %) and Orowan strengthening (10 %), since the contribution trend for strength coincides with

Table 5. Contribution of strengthening mechanisms and calculated values for the AM60/5wt.%Al₂O_{3p} MMC after 4 passes

Symbol	Description	Percentage of	
		Value	strengthening contribution
$\Delta\sigma_D$	enhancement of composite strength due to dislocation density increase	159 MPa	56 %
$\Delta\sigma_{\text{Hall-Petch}}$	enhancement of composite strength due to grain refining	98 MPa	34 %
$\Delta\sigma_{\text{Orowan}}$	enhancement of composite strength due to Orowan strengthening	28 MPa	10 %

that of hardness. According to the study of Sanaty-Zadeh [29], those composites in which the temperature of the process is at room temperature, the Orowan strengthening has higher values than the coefficient of thermal expansion (CTE) mismatch effect, while for those with a process temperature higher than room temperature ($\sim 270^\circ\text{C}$), the CTE mismatch effect becomes more significant than the Orowan strengthening. The effect of CTE mismatch between the matrix and reinforcement particles becomes most important as the temperature raises up, which results in an increase in dislocation density near the matrix-particle interface. From the present results of strengthening contribution calculation, it follows that the dislocation density increase strengthening due to thermal expansion mismatch has the stronger effect on hardness strengthening of MMCs under high temperature process, than those of Hall-Petch strengthening and Orowan strengthening.

The calculated results of contribution of hardness strengthening in Table 5 agree with the experimental results shown in Table 3, i.e., the contribution of ECAEed fine grain strengthening (Hall-Petch strengthening accompanied with dislocation density increase strengthening) is much higher than that of dispersion strengthening effect (Orowan strengthening).

4. Conclusion

This study proposes and investigates the microstructure and strengthening mechanism of nano-Al₂O_{3p} reinforced AM60 Mg based metal-matrix composites by ECAE. The present Mg-based MMCs are fabricated by the melt stirring technique. Based on the experimental results, the following conclusions and some important novelties could be drawn:

1. Severe plastic deformation by equal channel angular extrusion technique is shown to efficiently enhance the hardness of AM60 MMC due to its grain structural refinement.

2. Observing the microstructures of MMCs, the more uniform microstructure consisting of grains with an average grain size of $\sim 0.8\ \mu\text{m}$ is observed in the AM60/5wt.%Al₂O_{3p} MMC after 4 passes.

3. The hardness of MMCs increases evidently with

the increase of weight percentage of Al₂O_{3p} additions and ECAE passes.

4. The hardness of MMCs increases evidently with the increase of weight percentage of Al₂O_{3p} additions and ECAE passes. The optimal hardness of AM60/5wt.%Al₂O_{3p} MMC after 4 passes increased to 103.7 HV, which is by 87.2 % higher than that of as-cast AM60.

5. According to the calculation of the three strengthening mechanisms from all present parameters, the most important contribution is the dislocation density increase strengthening.

Acknowledgements

Authors thank Prof. P. W. Kao (National Sun Yat-Sen University, Taiwan) for his help in the work with an equal channel angular extrusion technique equipment.

References

- [1] Lin, P.-C. Huang, S.-J., Hong, P.-S.: *Acta Metall Slovaca*, 16, 2010, p. 237.
- [2] Huang, S.-J., Chen, Z.-W.: *Acta Metall Slovaca*, 16, 2010, p. 246.
- [3] Huang, S.-J., Chen, Z.-W.: *Kovove Mater*, 49, 2011, p. 259.
- [4] Saravanan, R. A., Surappa, M. K.: *Mater. Sci. Eng., A*, 276, 2000, p. 108. [doi:10.1016/S0921-5093\(99\)00498-0](https://doi.org/10.1016/S0921-5093(99)00498-0)
- [5] Cai, Y., Tan, M. J., Shen, G. J., Su, H. Q.: *Mater. Sci. Eng., A*, 282, 2000, p. 232. [doi:10.1016/S0921-5093\(99\)00707-8](https://doi.org/10.1016/S0921-5093(99)00707-8)
- [6] Ho, K. F., Gupta, M., Srivatsan, T. S.: *Mater. Sci. Eng., A*, 369, 2004, p. 302. [doi:10.1016/j.msea.2003.11.011](https://doi.org/10.1016/j.msea.2003.11.011)
- [7] Rogathi, P. K.: *Cast metal-matrix composites. ASM handbook-castings*, 15, 1992, p. 840.
- [8] Zrnik, J., Dobatkin, S. V., Mamuzic, I.: *METABK*, 47, 2008, p. 211.
- [9] Adedokun, S. T.: *Journal of Emerging Trends in Engineering and Applied Sciences*, 2, 2011, p. 360.
- [10] Hassan, S. F., Gupta, M.: *J. Alloys Compd.*, 419, 2006, p. 84. [doi:10.1016/j.jallcom.2005.10.005](https://doi.org/10.1016/j.jallcom.2005.10.005)
- [11] Hassan, S. F., Gupta, M.: *Mater. Sci. Eng., A*, 392, 2005, p. 163. [doi:10.1016/j.msea.2004.09.047](https://doi.org/10.1016/j.msea.2004.09.047)
- [12] Paramsothy, M., Hassan, S. F., Srikanth, N., Gupta M.: *Mater. Sci. Eng., A*, 527, 2009, p. 162. [doi:10.1016/j.msea.2009.07.054](https://doi.org/10.1016/j.msea.2009.07.054)

- [13] Paramsothy, M., Nguyen, Q. B., Tun, K. S., Chan, J., Kwok, R., Kuma, J. V. M., Gupta, M.: *J. Alloys Compd.*, 506, 2010, p. 600.
[doi:10.1016/j.jallcom.2010.07.123](https://doi.org/10.1016/j.jallcom.2010.07.123)
- [14] Habibnejad-Korayem, M., Mahmudi, R., Poole, W. J.: *Mater. Sci. Eng., A*, 519, 2009, p. 198.
[doi:10.1016/j.msea.2009.05.001](https://doi.org/10.1016/j.msea.2009.05.001)
- [15] Chen, T. J., Jiang, X. D., Ma, Y., Li, Y. D., Hao, Y.: *J. Alloys Compd.*, 496, 2010, p. 218.
[doi:10.1016/j.jallcom.2010.03.002](https://doi.org/10.1016/j.jallcom.2010.03.002)
- [16] Semenov, V. I., Jeng, Y.-R., Huang, S.-J., Dao, Y.-Zh., Hwang, S.-J., Shuster, L. Sh., Chertovskikh, S. V., Lin, P.-C.: *J. Frict. Wear*, 30, 2009, p. 194.
[doi:10.3103/S1068366609030088](https://doi.org/10.3103/S1068366609030088)
- [17] Jiang Jufu, Wang Ying, Qu Jianjun, Du Zhiming, Sun Yi, Luo Shoujing: *J. Alloys Compd.*, 497, 2010, p. 62.
[doi:10.1016/j.jallcom.2010.02.099](https://doi.org/10.1016/j.jallcom.2010.02.099)
- [18] Ding, S. X., Lee, W. T., Chang, C. P., Chang, L. W., Kao, P. W.: *Scripta Mater.*, 59, 2008, p. 1006.
[doi:10.1016/j.scriptamat.2008.07.007](https://doi.org/10.1016/j.scriptamat.2008.07.007)
- [19] Furukawa, M., Horita, Z., Langdon, T. G.: *Mater. Sci. Eng., A*, 332, 2002, p. 97.
[doi:10.1016/S0921-5093\(01\)01716-6](https://doi.org/10.1016/S0921-5093(01)01716-6)
- [20] Humphreys, F. J., Hatherly, M.: *Recrystallization and Related Annealing Phenomena*. 2nd ed. Oxford, Elsevier 1996.
- [21] Mackenzie, L. W. F., Lorimer, G. W., Humphreys, F. J., Wilks, T.: *Mater. Sci. Forum*, 467–470, 2004, p. 477.
[doi:10.4028/www.scientific.net/MSF.467-470.477](https://doi.org/10.4028/www.scientific.net/MSF.467-470.477)
- [22] Godon, A., Creus, J., Cohendoz, S., Conforto, E., Feaugas, X., Girault, P., Savalla, C.: *Scripta Mater.*, 62, 2010, p. 403. [doi:10.1016/j.scriptamat.2009.11.038](https://doi.org/10.1016/j.scriptamat.2009.11.038)
- [23] Zhao, Y. T., Zhang, S. L., Chen, G., Cheng, X. N., Wang, C. Q.: *Compos. Sci. Technol.*, 68, 2008, p. 1463.
[doi:10.1016/j.compscitech.2007.10.036](https://doi.org/10.1016/j.compscitech.2007.10.036)
- [24] Hassan, S. F., Gupta, M.: *Mater. Sci. Technol.*, 20, 2004, p. 1383. [doi:10.1179/026708304X3980](https://doi.org/10.1179/026708304X3980)
- [25] Hassan, S. F., Gupta, M.: *J. Compos. Mater.*, 41, 2007, p. 2533. [doi:10.1177/0021998307074187](https://doi.org/10.1177/0021998307074187)
- [26] Ashby, M. F., Jones, D. R. H.: *Engineering Materials 1*. Oxford, Pergamon Press 1980.
- [27] Goh, C. S., Wei, J., Lee, L. C., Gupta, M.: *Acta Mater.*, 55, 2007, p. 5115. [doi:10.1016/j.actamat.2007.05.032](https://doi.org/10.1016/j.actamat.2007.05.032)
- [28] Zhang, Z., Chen, D. L.: *Mater. Sci. Eng., A*, 483, 2008, p. 148. [doi:10.1016/j.msea.2006.10.184](https://doi.org/10.1016/j.msea.2006.10.184)
- [29] Sanaty-Zadeh, A.: *Mater. Sci. Eng., A*, 531, 2012, p. 112. [doi:10.1016/j.msea.2011.10.043](https://doi.org/10.1016/j.msea.2011.10.043)